Int J Thermophys (2018) 39:24
https://doi.org/10.1007/s10765-017-2345-0

ICPPP 18

Thermal Diffusivity of High-Density Polyethylene Samples of Different Crystallinity Evaluated by Indirect Transmission Photoacoustics

M. Nesic[1,2] · M. Popovic[2] · M. Rabasovic[3] · D. Milicevic[2] · E. Suljovrujic[2] · D. Markushev[3] · Z. Stojanovic[2]

Received: 14 October 2015 / Accepted: 5 December 2017 / Published online: 18 December 2017

Abstract In this work, thermal diffusivity of crystalline high-density polyethylene samples of various thickness, and prepared using different procedures, was evaluated by transmission gas-microphone frequency photoacoustics. The samples' composition analysis and their degree of crystallinity were determined from the wide-angle X-ray diffraction, which confirmed that high-density polyethylene samples, obtained by slow and fast cooling, were equivalent in composition but with different degrees of crystallinity. Structural analysis, performed by differential scanning calorimetry, demonstrated that all of the used samples had different levels of crystallinity, depending not only on the preparing procedure, but also on sample thickness. Therefore, in order to evaluate the samples' thermal diffusivity, it was necessary to modify standard photoacoustic fitting procedures (based on the normalization of photoacoustic amplitude and phase characteristics on two thickness levels) for the interpretation of photoacoustic measurements. The calculated values of thermal diffusivity were in the range of the expected literature values. Besides that, the obtained results indicate the unexpected correlation between the values of thermal diffusivity and thermal conductivity with the degree of crystallinity of the investigated geometrically thin samples. The results indicate the necessity of additional investigation of energy transport in

This article is part of the selected papers presented at the 18th International Conference on Photoacoustic and Photothermal Phenomena.

✉ M. Nesic
mioljub@gmail.com; mioljub.nesic@vin.bg.ac.rs

1 School of Electrical Engineering, University of Belgrade, Bul. kralja Aleksandra 73, Belgrade 11120, Serbia

2 Vinca Institute of Nuclear Sciences, University of Belgrade, PO Box 522, Belgrade 11001, Serbia

3 Institute of Physics, University of Belgrade, Pregrevica 118, Belgrade-Zemun 11080, Serbia

macromolecular systems, as well as the possible employment of the photoacoustic techniques in order to clarify its mechanism.

Keywords Crystallinity · HDPE · Multi-parameter fitting · Photoacoustics · Photothermal · Thermodynamics

1 Introduction

Polyethylene (PE) is well known and one of the most frequently used polymers. Its universal value is proven throughout its whole lifespan—from its straightforward and easily adoptable industrial production process to the myriad of application fields, depending on the type, i.e., on its physical and chemical properties [1–3]. The material of interest in this work is high-density polyethylene (HDPE), the type of PE characterized by low degree of branching (which results in linear molecule packing with stronger intra-molecular bonds) and relatively high density and level of crystallinity compared to other PEs [4–9]. Due to excellent impact resistance, high tensile strength, low moisture absorption and chemical resistance, HDPE is used in a variety of applications such as product packaging, piping production, electrical insulation, as well as in many other plastic product industries [1,10,11].

In all of these applications, it is of great importance to be familiar with experimentally evaluated thermal properties of HDPE as well as with their relation to the structure of macromolecular materials and dynamic processes in them, in order to achieve the engineering of these properties for the specific applications [1]. These experimental investigations are also significant from the point of view of fundamental research of energy transport mechanism through macromolecular systems [12,13]. In recent decades, dynamic thermal properties have been investigated by photothermal (PT) and photoacoustic (PA) methods, and the results have shown good agreement with literature values, obtained by other methods [12,14–19]. This fact represents an encouragement for further application of PT/PA methods in thermal characterization of polymer materials, but also the stimulus for their further development, including inverse procedures, in order to provide a better explanation between structural changes, thermal properties and energy transport mechanisms of these materials.

In this paper, thermal diffusivity of crystalline HDPE films, of various thickness and prepared using different procedures, is examined using transmission gas-microphone PA frequency method. In the first part of the work, the preparation procedure of the samples is presented in brief, along with the results and the discussion of the examination performed by wide-angle X-ray diffraction (WAXD) and differential scanning calorimetry (DSC) techniques. After that, the measured PA responses, both amplitude and phase, are displayed. The analysis of WAXD and DSC results indicates that the processing of PA measurements, based on the normalization of amplitude and phase characteristics to two thickness levels, must be modified. In the second part, the developed inverse procedure for the evaluation of thermal properties from the PA measurements is explained, and the obtained results are presented in table form. Finally, the most important conclusions are drawn.

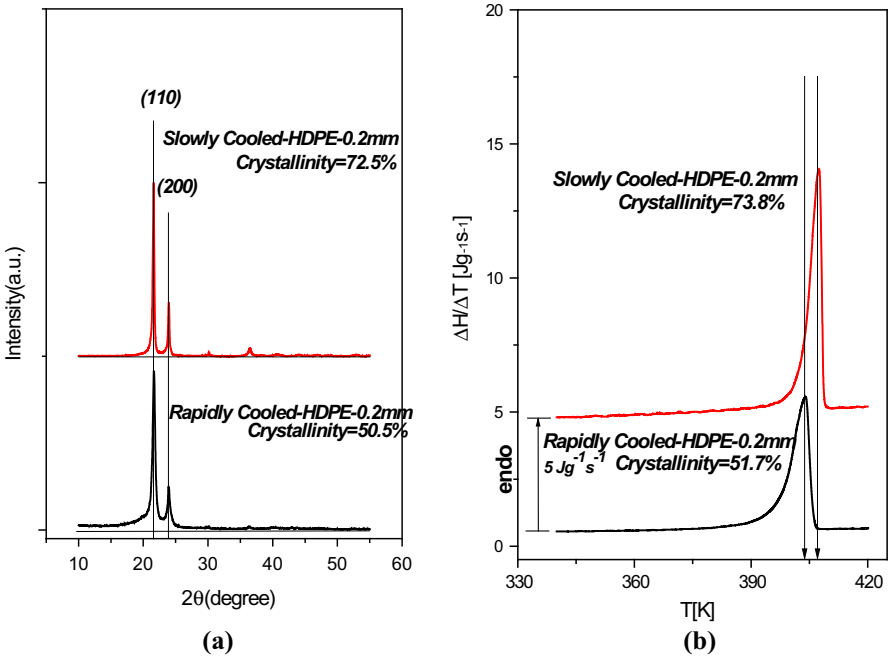

Fig. 1 The results of (a)WAXD and (b) DSC measurements

2 Experiment

2.1 Preparation of Samples and Results of WAXD and DSC Measurements

The polymer used in the present study was HDPE Hiplex HHM 5502 (ρ = 0.955 g cm^{-3}, M_w = 300 000). Square-shaped isotropic sheets of different thickness (200 μm, 400 μm and 600 μm) were obtained by 20 min compression molding in a Carver laboratory press at 160 °C and with gradual pressure increment, up to 3.28 MPa. One set of the molded sheets was rapidly cooled by swift sinking in the mixture of ice and water (∼ 0 °C), in order to obtain samples with low level of crystallinity. The other set was prepared by slow cooling from melting temperature to room temperature (∼ 20 °C), keeping the samples between the press platens without pressure for the period of 6 h, thus attaining samples of high crystalline content. The composition of PE samples obtained by these two different preparing procedures was determined from WAXD measurements, using a Bruker D8 Advance Diffractometer (in normal mode, with Cu Kα emission). Parallel beam optics was adjusted by a parabolic Göbel mirror (push plug Ni/C) with horizontal grazing incidence soller slit of 0.12° and a LiF monochromator. Diffractometer scans were taken within the angular range of 2θ = 10°–45°, at steps of 0.02°, with the 10 s exposition step (see Fig. 1a for the thinnest samples). Stationary thermal properties of all samples were obtained by DSC, using a PerkinElmer DSC-7 differential scanning calorimeter with nitrogen as the purge gas. Samples weighing 7–8 mg were analyzed by heating from 320 K to 450 K at the

Table 1 Crystallinity as a function of preparation conditions and thickness of the sample

χ (%)	200 μm		400 μm	600 μm
	DSC	WAXD	DSC	DSC
Fast cooled	51.7	50.5	57.4	59.3
Slowly cooled	73.8	72.5	71.5	70.8

rate of 10 K min^{-1}, and their heats of fusion (ΔH_f) were derived (see Fig. 1b for the thinnest samples). From the DSC measurements, the degree of crystallinity (DoC) was calculated as $\chi = \Delta H_f / \Delta H_{f0}$, where $\Delta H_{f0}$is the heat of fusion of a perfectly crystalline PE sample ($\Delta H_{f0} = 289\,J\,g^{-1}$) [1,20]; from the WAXD measurements, the DoC was evaluated from the diffraction patterns by resolving multiple peak data into individual crystalline peaks and an amorphous halo [21,22]. Quantitative analysis was performed using a standard software package for fitting the experimental spectra.

The results of the analysis of DSC and WAXD measurements are summarized in Table 1.

It can be observed, from Table 1, that in slowly cooled samples crystallinity is higher (around 70 %, compared to the rapidly cooled ones, where it is around 50 %) and is slightly growing as the sample thickness decreases (around 3 %, overall). In rapidly cooled samples, the opposite trend is present: the crystallinity falls with the decrease in sample thickness (around 7.5 %, overall). Higher degree of crystallinity in slowly cooled samples is related to the longer period of cooling, during which the parts of the macromolecule chain have sufficient time to line up more regularly. The difference in the influence of sample thickness on the crystallinity between slowly and rapidly cooled samples can be related to the greater influence of surface effects in slowly cooled ones. Namely, the production of crystalline materials from the melting via rapid cooling introduces defect centers at surface. The influence of defect centers on thermal properties is more pronounced in thinner samples, in particular, because the defect centers decrease the mean free path of thermal energy carriers.

2.2 PA Experiment and Evaluation of Thermal Diffusivity

The samples, both slowly and rapidly cooled ones, at three levels of thickness—l_s = 200 μm, 400 μm, 600 μm—were made disk-shaped (r = 5 mm), and a thin absorption layer (∼10 μm) was deposited using the air-brush technique. They were put into a minimum volume PA cell [23], which is part of a larger instrument used for PA frequency response measurements.

The instrument setup consists of a detection unit and a signal processing/power supply unit (a box containing batteries and home-made electronics, Fig. 2a). The setup also contains a PC, with the appropriate acquisition software and a stereo input sound card, acting as a lock-in amplifier. The modulation signal, representing the input to the driver, which controls the operation of the laser/LED, comes from the sound card line-out connector (standard 3.5 mm stereo connector, Fig. 2b). The reference signal from the photodiode, carrying the information about the input source power and phase as well, is amplified ten times, while the microphone signal is amplified 10

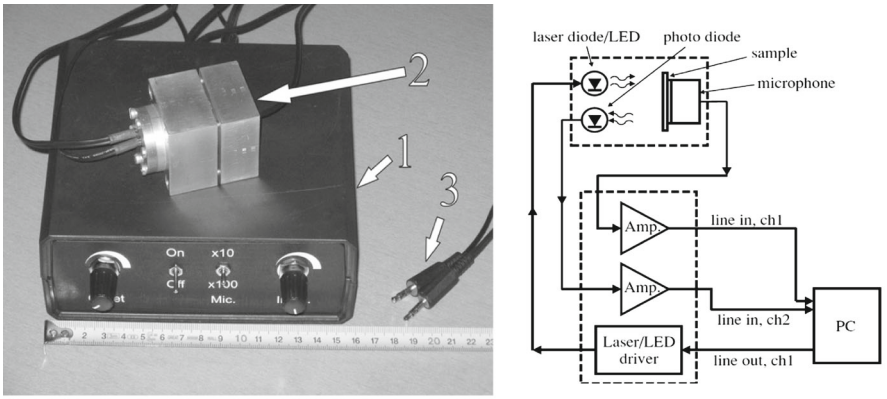

Fig. 2 Experimental setup: (a) Photograph of the apparatus: 1—The box which contains the electronics and the batteries, 2—PA cell, 3—standard 3.5 mm stereo connectors; (b) Schematic diagram—the PA cell marked with the dotted line.

(or 100) times—all achieved by the use of a set of low-noise, high-speed operational amplifiers OP37. This type of amplifier has demonstrated a flat amplitude response in the 10 Hz–20 kHz frequency range, showing no phase change. Both signals are processed by the two line-in stereo connector channels of the sound card [24].

The PA cell is made from duralumin, with the electret microphone (ECM60, 9.8 mm in diameter, 2.5 mV Pa^{-1} of sensitivity), laser diode/LED and photodiode (all replaceable) embedded in it. It is a *minimum volume* type cell, with the interior of the microphone (confined with its orifice on one and its diaphragm on the other end) acting as the PA cell chamber—the configuration that guarantees high sensitivity and low level of losses [23,24]. The absorption layer, which plays a significant role as the absorber of electromagnetic (EM) energy and the light radiation protector for the microphone, is illuminated ("PA transmission configuration") and is considered a surface heat source for the sample, whose influence on heat transfer and consequently to the PA response can be neglected [14–19].

Experimentally obtained values of amplitude and phase PA response of both rapidly cooled and slowly cooled HDPE, at all three thickness levels, are presented in Fig. 3.

In order to make a connection between the thermoelastic (TE) properties of a single-layered sample and its PA response, the composite piston theoretical model is deployed where the sample is modeled as a simply supported plate [25–27]. This model predicts that the resulting pressure, in theory, is the sum of two components, namely p_{th}—the component that originates from the periodic expansion of a thin gas layer closest to the sample—and p_{ac}—the component which sums up all the TE movements inside the sample and on its surface (Eq. 1):

$$\tilde{p} = \tilde{p}_{th} + \tilde{p}_{ac} \quad \rightarrow \quad \begin{aligned} \tilde{p}_{th} &= \frac{\gamma P_0}{l_a T_0} \int_{l_s}^{l_s + 2\pi\mu_a} \tilde{\vartheta}_s(l_s) e^{-\tilde{\sigma}_a(x-l_s)} dx, \\ \tilde{p}_{ac} &= \frac{3\gamma P_0}{l_a} \alpha_S \frac{R^2}{l_s^3} \int_0^{l_s} (x - \tfrac{l_s}{2}) \tilde{\vartheta}_s(x) dx. \end{aligned} \tag{1}$$

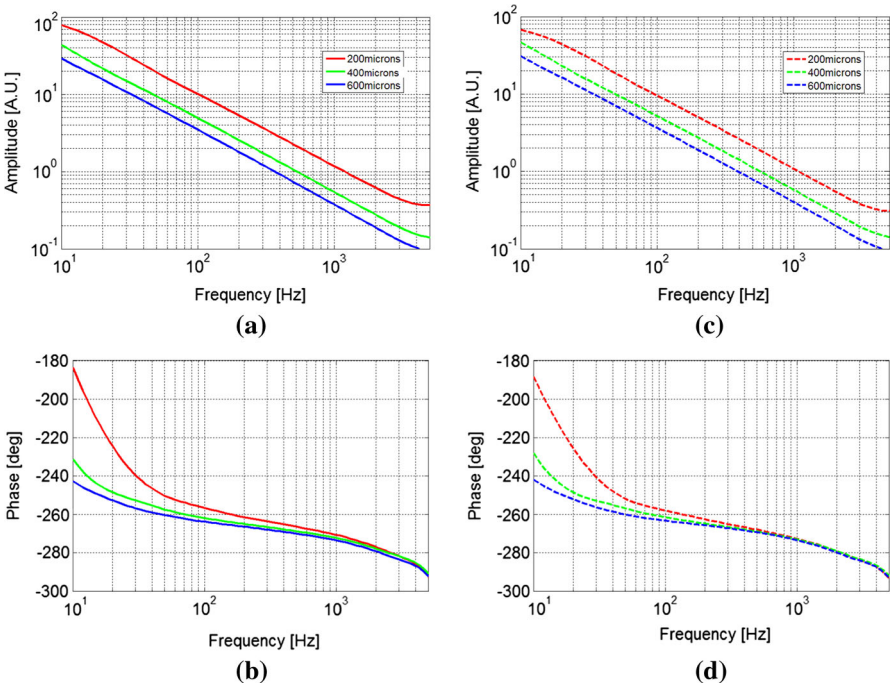

Fig. 3 Experimental results: rapidly cooled samples (low crystalline) on the left, amplitude and phase (*a* and *b*, respectively), and slowly cooled ones () on the right, amplitude and phase (*c* and *d*, respectively)

Here, γ annotates the adiabatic coefficient, P_0 is the atmospheric pressure, l_a is the length of the gas column inside the PA chamber, while T_0 stands for the room temperature. Furthermore, α_S is the linear coefficient of thermal expansion of the sample, R is its radius, while l_s annotates its thickness. The symbols $\tilde{\vartheta}_s$ and μ_a represent the distribution of temperature variations across the sample and the thermal diffusion length in the air (gas). These equations, when solved (and having accounted for the influence of thermal memory effect on the distribution of temperature variations in the sample and its environment) take their final form [28,29]:

$$\begin{aligned} \tilde{p}_{th} &= \frac{\gamma P_0 S_0}{T_0} \frac{\tilde{Z}_{cs}}{\tilde{\sigma}_a l_a} \frac{1}{\sinh(\tilde{\sigma}_s l_s)}, \\ \tilde{p}_{ac} &= 6\gamma P_0 S_0 \alpha_s \frac{R^4}{R_c^2 l_a l_s} \tilde{Z}_{cs} \frac{\cosh(\tilde{\sigma}_s l_s) - \frac{\tilde{\sigma}_s l_s}{2} \sinh(\tilde{\sigma}_s l_s) - 1}{(\tilde{\sigma}_s l_s)^2 \sinh(\tilde{\sigma}_s l_s)}. \end{aligned} \tag{2}$$

In the above expressions, S_0 stands for the surface heat source, which equals half of the excitation energy intensity, R_c represents the radius of the circle where the sample is *simply supported*, $\tilde{\sigma}_i$ and $\tilde{Z}_{ci}$, $i = a, s$ are the heat wave vector and the thermal impedance of the environment (air or sample), given by:

$$\begin{aligned} \tilde{\sigma}_i &= \frac{1}{\sqrt{D_{Ti}}} \sqrt{j\omega(1 + j\omega\tau_i)}, \\ \tilde{Z}_{ci} &= \frac{\sqrt{D_{Ti}}}{k_i} \sqrt{\frac{(1 + j\omega\tau_i))}{j\omega}}, \end{aligned} \tag{3}$$

where k_i, and $D_{Ti} \quad i = a, s$, stand for the thermal conductivity. The radial modulation frequency is $\omega = 2\pi$ f, and $\tau_i, \quad i = a, s$, is the parameter which describes the influence of thermal memory of the medium, referred to as *thermal relaxation time* [28–31].

The appearance of the parameter τ_i in this work is the consequence of the use of the *generalized model of photothermal wave propagation* [30]. However, the comparisons of the experimental measurement in Fig. 3 to earlier theoretical investigations which include thermal memory effects [28–31], and also to previously obtained experimental measurements on certain plastics in the frequency range up to 1 kHz [14–19], lead us to the conclusion that τ_i is small enough and that its influence can be neglected in the measured frequency range.

3 Self-Consistent Inverse PA Procedure: Results and Discussion

The results of DSC and WAXD analysis (Table 1) implied that, in both rapidly and slowly cooled set of samples, not a single pair of samples with the same crystallinity could be identified! Therefore, we had to presume that not two samples, structurally the same but of the different thickness, could be found. Consequently, the standard procedure of normalizing the results to two thickness levels, although widely adopted in solving inverse PA problems [14,32,33], could not be deployed for the samples obtained by the described process. That is why our own system of evaluating thermal parameters from the measured PA response had to be developed.

In HDPE and macromolecular materials, the contribution of the p_{th} component is significant at very low frequencies (under 50Hz), and in this region microphone transfer characteristic is no longer flat [34]. However, in the measurement range 100 Hz–1 kHz, where the influence of the measurement chain on the shape of the signal is considered negligible, the dominance of the TE component of the PA response is crucial [14]. So, basing our concept on the experimental data shown in Fig. 3, and on the detailed analysis of the model [35] given by Eq. 2 which can be found in the literature [34], the model is simplified as:

$$\tilde{p}_{TE}^{(HF)} = P_0 I_0 \frac{\gamma}{l_a} \cdot \frac{3\alpha_s R^4}{4k_s R_c^2} \cdot \frac{1}{x}\left(1 - \frac{1}{\sqrt{x}}\right) \cdot \exp\left(-i\left[\frac{3}{2}\pi - \frac{1}{\sqrt{x}}\right]\right),$$
$$x = \frac{\pi f}{D_{Ts}} l_s^2$$

where

$$\left|\tilde{p}_{TE}^{(HF)}\right| = P_0 I_0 \frac{\gamma}{l_a} \cdot \frac{3\alpha_s R^4}{4k_s R_c^2} \cdot \frac{1}{x}\left(1 - \frac{1}{\sqrt{x}}\right),$$
$$\arg(\tilde{p}_{TE}^{(HF)}) = \frac{3}{2}\pi - \frac{1}{\sqrt{x}}, \tag{4}$$

although the four unknown properties of the sample still influence the PA response in the measurement range: (1) thermal conductivity (k_s[W · m^{-1} · K^{-1}]), (2) thermal

Table 2 Literature and fitted values of HDPE's thermodynamic parameters

	Intervals
HDPE—high-density polyethylene	
k_s thermal conductivity $\left[\frac{W}{m \cdot K}\right]$	0.33–0.53
D_{Ts} thermal diffusivity $D_{Ts} = \frac{k_s}{C_p} = \frac{k_s}{c \cdot \rho}$, $\left[\times 10^{-6}\ \frac{\mathrm{m}^2}{h} boxs\right]$	(0.265–0.313)

diffusivity ($D_{Ts}[\mathrm{m}^2 \cdot \mathrm{s}^{-1}]$), (3) linear expansion coefficient ($\alpha_s[\mathrm{K}^{-1}]$) and (4) sample thickness (l_s[m]). Fortunately, the phase characteristic depends only on thermal diffusivity and sample thickness. Having this in mind, a rough fitting of the phase characteristic was done and a range of values for D_{Ts} of the used samples was obtained, which is presented in Table 2, along with the range of literature values of k_s. The value of $\alpha_s = 225 \cdot 10^{-6}\,\mathrm{K}^{-1}$ was found in the literature, too [36,37].

Intervals of k_s and D_{Ts} are presented by five equidistant points, which are put into the computing program, written in Matlab, and twenty-five theoretical PA response vectors are derived (over the experimental frequency range), each corresponding to the exact set of parameters (k_s, D_{Ts}). Then, the standard deviation (StD) from the experimental data is computed on the defined region of interest (RoI) for each vector; the minimum value of the calculated StD determines the theoretical vector, based on the set of parameters ($k_s D_{Ts}$) which are closest to the set corresponding to the actual, experimentally measured data. The calculated StD values are mapped on the $k_s - D_{Ts}$ plane as 3D mesh-figures (Figs. 4, 5), and this procedure is repeated for each sample thickness level (200 μm, 400 μm, 600 μm), for both rapidly and slowly cooled samples. The evaluated sets of (k_s, D_{Ts}) parameters, corresponding to each of the minima, are presented in Table 3.

The comparison of literature and roughly fitted thermal parameter values (Table 2) with ($k_s D_{Ts}$) obtained parameter set (Table 3) indicates the high level of compliance [14,18,36,37].

As can be clearly observed in Fig. 4, the two thick sets of samples (at 400 μm and 600 μm) show no observable differences, when it comes to the evaluation of (k_s,D_{Ts}) parameters (Table 2). On the other hand, in thinnest samples (at 200 μm), these characteristics emerge in Fig. 5, where the minima of the *StD*-planes are clearly not the same, and, consequently, the (k_s, D_{Ts}) parameter sets are different, too (Table 3, data given in bold). In thinnest samples, both slowly and rapidly cooled ones, the increase in thermal conductivity is observed in comparison with thicker samples. This result is not expected if thermal energy carriers are considered to be phonons. The observed rise is larger in slowly cooled (more crystalline) samples than in rapidly cooled (less crystalline) ones, which is expected. On the other hand, in slowly cooled samples, thermal diffusivity remains intact, regardless of the thickness and is the same as in two thick, slowly cooled ones. The thinnest rapidly cooled sample exerts the decrease of thermal diffusivity, which is in accordance with expectations.

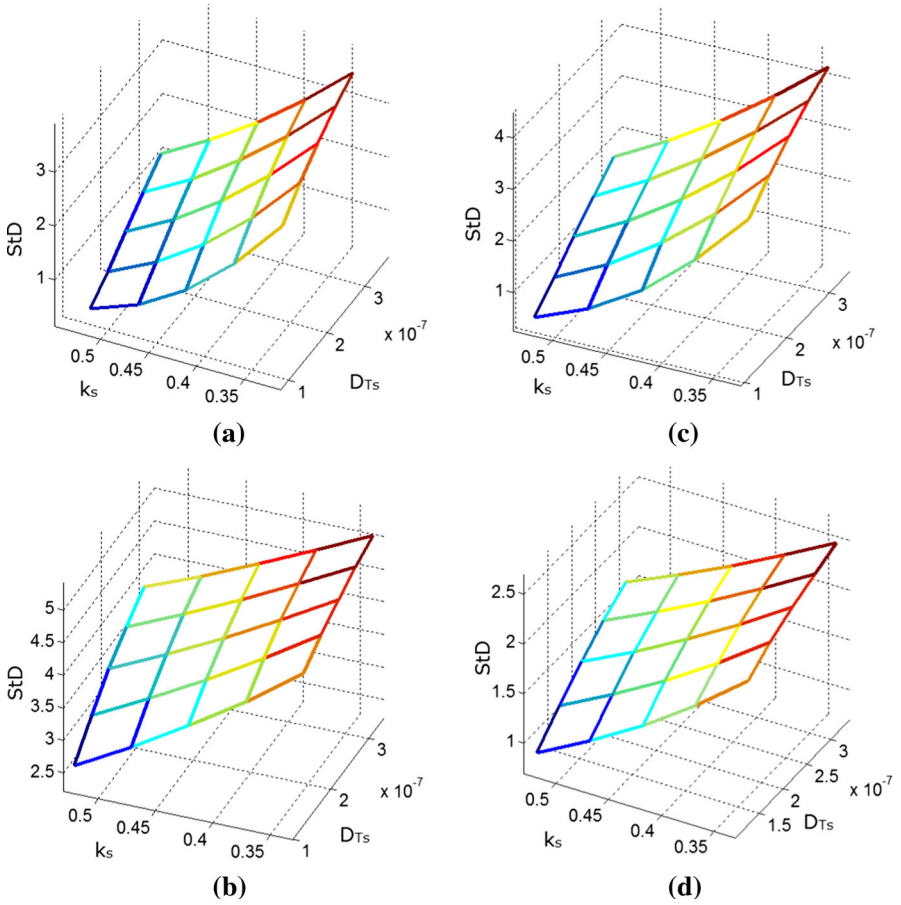

Fig. 4 Comparison of the computed StD over RoI as the function of (k_s, D_{Ts}) sets, for the samples 400 μm and 600 μm thick: rapidly cooled samples on the left (low crystalline, *a* and *b*, respectively), slowly cooled on the right (highly crystalline, *c* and *d*, respectively)

From Table 3, it can be remarked that thermal parameters obtained by amplitude and phase fitting do not correlate with the degree of crystallinity (DoC) of thicker samples (400 μm and 600 μm), notwithstanding the way of their preparation. However, this correlation exists in both thin samples, meaning that PA transmission method could be employed for the DoC determination of the samples thinner or equal to 200 μm only.

In rapidly cooled samples, the fall of crystallinity is correlated with the rise of thermal conductivity (Tables 1, 3), which contradicts the conclusions of [14,18]. In slowly cooled samples, the rise of the DoC is correlated with the rise of thermal conductivity (Tables 1, 3), which is in accordance with results from [18]. However, our results indicate the correlation of crystallinity falls in rapidly cooled samples with thermal diffusivity decrease, meaning that less crystalline samples have higher volumetric thermal capacity, which is also contradictory to the results of [18]. The

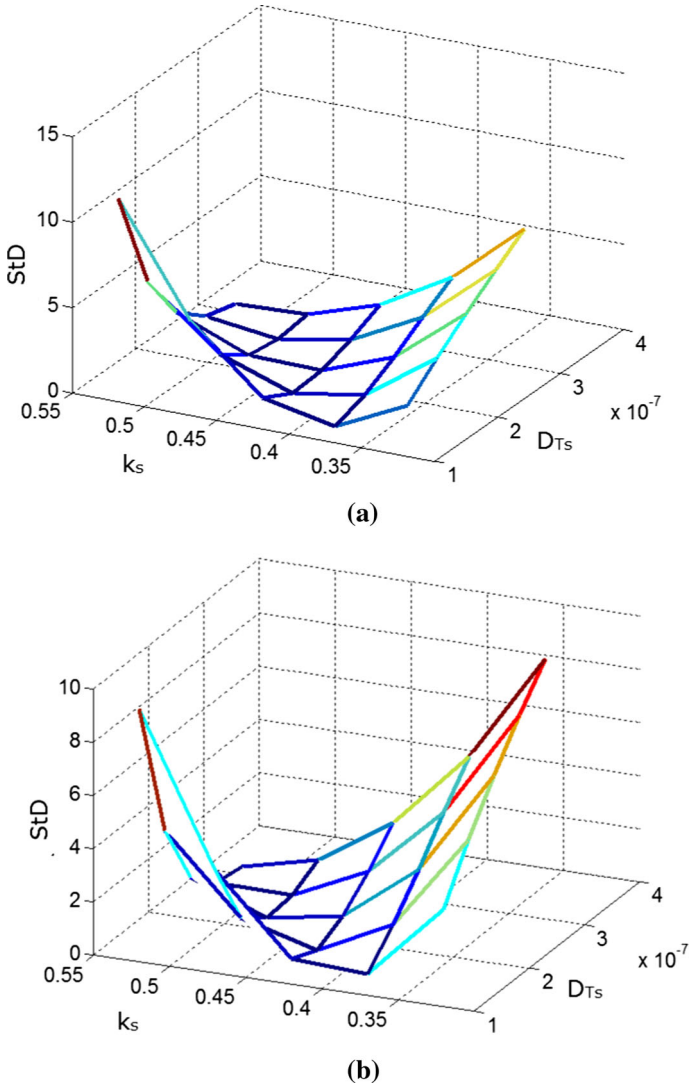

Fig. 5 Comparison of the computed StD over RoI as the function of (k_s, D_{Ts}) sets, for the samples 200 μm thick—highly and low crystalline (*a* and *b*, respectively)

assumption of an alternative approach to heat transfer is supported in some papers dealing with polaron-assisted heat transfer mechanism in macromolecular chains [38].

Throughout the literature, however, in PA measurements, thin aluminum foil was used as optical absorption layer, while in our measurements it was the dye. Besides the heat transfer mechanism, the observed phenomena could be attributed to the influence of the absorption layer on the TE component of the PA response.

Both of these possibilities represent the subject of our current research.

Table 3 Evaluated values of HDPE's thermodynamic parameters, with uncertainty estimated as the half-distance between the points

Thickness [μm]		HDPE—high-density polyethylene		
		Fast cooled	Slowly cooled	Uncertainty
400, 600	$k_s \left[\frac{W}{m \cdot K}\right]$	0.33	0.33	(±0.02)
	$D_{Ts} \left[\times 10^{-6} \frac{m^2}{s}\right]$	0.313	0.313	(±0.019)
200	$k_s \left[\frac{W}{m \cdot K}\right]$	**0.48**	**0.53**	(±0.02)
	$D_{Ts} \left[\times 10^{-6} \frac{m^2}{s}\right]$	**0.265**	**0.313**	(±0.019)

Finally, it should be stressed out that all the values of thermal conductivity and thermal diffusivity obtained by the developed self-consistent inverse procedure fall within the range of literature values presented in Table 2.

4 Conclusions

The first conclusion of this paper is that, in the process of the estimation of thermal parameters in macromolecular materials, the inverse procedure, based on the normalization of the recorded amplitude and phase characteristics, should be modified. Moreover, the modification is suggested which consists of the PA response model approximation and the fitting of both amplitude and phase characteristics, in order to augment the accuracy of the parameter estimation.

Second, the employment of the suggested inverse procedure results in obtaining the values of thermal conductivity and thermal diffusivity which highly correlate with the literature values.

Third, by investigating two groups of HDPE samples (with low and high level of DoC) it is shown that the correlation between thermal parameters and crystallinity can be established in samples of 200 μm and thinner only, stressing out the possibility of employing the photoacoustics in the determination of the DoC of thin polymer films.

Finally, different tendencies in correlating thermal parameters with crystallinity are noticed in rapidly cooled (low crystalline) and slowly cooled (highly crystalline) thin samples, demanding more scrutiny in further explorations, both theoretical and experimental, which is the subject of our future work in this area.

Acknowledgements Authors wish to acknowledge the support of Ministry of Education and Science of the Republic of Serbia throughout the research project III-45005, OI-171016 and 172026.

References

1. B. Wunderlich, *Thermal Analysis of Polymeric Materials* (Springer, Berlin, 2005)
2. T.C.M. Chung, Macromolecules **46**, 6671–6698 (2013)
3. A.A. Basfar, J. Mosnáček, T.M. Shukri, M.A. Bahattab, P. Noireaux, A. Courdreuse, J. Appl. Polym. Sci. **107**, 642–649 (2008)

4. S. Galovic, B. Secerov, S. Trifunovic, D. Milicevic, E. Suljovrujic, Radiat. Phys. Chem. **81**, 1374–1377 (2012)
5. D. Milicevic, M. Micic, G. Stamboliev, A. Leskovac, M. Mitric, E. Suljovrujic, Fibers Polym. **13**, 466–470 (2012)
6. D. Milicevic, S. Trifunovic, M. Popovic, T. Vukasinovic Milic, E. Suljovrujic, Nucl. Instrum. Methods B **260**, 603–612 (2007)
7. D. Milicevic, M. Micic, E. Suljovrujic, Polym. Bull. **71**, 2317–2334 (2014)
8. Q. Yuan, Y. Yang, J. Chen, V. Ramuni, R.D.K. Misra, K.J. Bertrand, Mater. Sci. Eng. A Struct **527**, 6699–6713 (2010)
9. E. Suljovrujic, M. Micic, D. Milicevic, J. Eng. Fibers Fabr. **8**, 131–143 (2013)
10. S. Kumar, A.K. Panda, R.K. Singh, Resour. Conserv. Recycl. **55**, 893–910 (2011)
11. M. Faizal, A. Bouazza, R.M. Singh, Renew. Sustain. Energy Rev. **57**, 16–33 (2016)
12. X. Zaoli, X. Shen, X. Tang, X. Wang, AIP Adv. **4**, 017131 (2014)
13. P.B. Allen, Phys. Rev. B **88**, 144302 (2013)
14. A.M. Mansanares, H. Vargas, F. Galembeck, J. Buijs, D. Bicanic, J. Appl. Phys. **70**, 7046–7050 (1991)
15. R. Sanchez, J. Rieumont, S. Cardoso, M. Silva, M. Sthel, M. Massunaga, C.N. Gatts, H. Vargas, J. Braz. Chem. Soc. **10**, 97–103 (1999)
16. A.C. Bento, D.T. Dias, L. Olenka, A.N. Medina, M.L. Baesso, Braz. J. Phys. **32**, 483–494 (2002)
17. L.H. Poley, A.P.L. Siqueira, M.G. da Silva, H. Vargas, Polímeros **14**, 8–12 (2004)
18. B. Bonno, J.L. Laporte, R. Tascon, R.T. D'Leon, Instrum. Sci. Technol. **33**, 151–160 (2005)
19. L.H. Poley, H. Vargas, M.G. da Silva, A.P.L. Siqueira, R. Sanchez, Polímeros **14**, 8–12 (2004)
20. B. Wunderlich, C.M. Cormier, J. Polym. Sci. A **2**, 987–988 (1967)
21. C.G. Vonk, J. Appl. Crystallogr. **6**, 148–152 (1973)
22. V. Jokanovic, Instrumental Methods: Key to Understanding Nanotechnologies and Nanomedicine, (Engineering Academy of Serbia: VINCA Institute for Nuclear Sciences, Belgrade, 2014—in Serbian) (title of the original: Instrumentalne metode ključ za razumevanje nanotehnologija i nanomedicine). ISBN 978-86-7306-123-8
23. L.F. Perondi, L.C.M. Miranda, J. Appl. Phys. **62**, 2955–2959 (1987)
24. M.D. Rabasovic, M.G. Nikolic, M.D. Dramicanin, M. Franko, D.D. Markushev, Meas. Sci. Technol. **20**, 095902 (2009)
25. G. Rousset, F. Lepoutre, L. Bertrand, J. Appl. Phys. **54**, 2383 (1983)
26. D.M. Todorovic, P.M. Nikolic, *Progress in Photothermal and Photoacoustic Science and Technology*, vol. 4, ed. by A. Mandelis (SPIE Press Book, 2000), p. 272. ISBN: 9780819435064
27. D.M. Todorovic, B. Cretin, Y.Q. Song, P. Vairac, J. App. Phys. **107**, 023516 (2010)
28. D. Markushev, M.D. Rabasovic, M. Nesic, M. Popovic, S. Galovic, Int. J. Thermophys. **33**, 2210–2216 (2012)
29. M. Nesic, P. Gusavac, M. Popovic, Z. Soskic, S. Galovic, Phys. Scr. **T149**, 014018 (2012)
30. S. Galovic, D. Kostoski, J. Appl. Phys. **93**, 3063–3070 (2003)
31. S. Galovic, Z. Soskic, M. Popovic, D. Cevizovic, Z. Stojanovic, J. Appl. Phys. **116**, 024901 (2014)
32. J.A. Balderas-Lopez, A. Mandelis, Rev. Sci. Instrum. **74**, 5219 (2003)
33. J.A. Balderas-Lopez, Rev. Sci. Instrum. **77**, 064902 (2006)
34. Z. Soskic, S. Ciric-Kostic, S. Galovic, Int. J. Therm. Sci. **109**, 217–230 (2016)
35. P.C. Hansen, Numer. Algorithms **6**, 1–35 (1994)
36. http://www.engineeringtoolbox.com/pipes-temperature-expansion-coefficients-d_48.html. Accessed 09 Nov 2017
37. http://www.maropolymeronline.com/Properties/HDPE%20Prop.asp. Acccessed 09 Nov 2017
38. D. Cevizovic, S. Galovic, A. Reshetnyak, Z. Ivic, Chin. Phys. B **22**, 060501 (2013)